HHS Public Access

Author manuscript

J Neuroophthalmol. Author manuscript; available in PMC 2024 June 01.

Published in final edited form as:

J Neuroophthalmol. 2023 June 01; 43(2): 220–226. doi:10.1097/WNO.0000000000001696.

Visual pathway involvement in NMDA receptor encephalitis: a clinical, optical coherence tomography, and 18-fluorodeoxyglucose PET/CT approach

Grigorios Kalaitzidis, M.D.[1], **Angeliki Filippatou, M.D.**[1], **Nicholas Fioravante, Bsc.**[1], **Alissa Rothman, M.D.**[1], **Elias S. Sotirchos, M.D.**[1], **Eleni Vasileiou, M.D.**[1], **Henrik Ehrhardt, MBBCh., MSc.**[1], **Agustina Quiroga, B.A.**[1], **Nicole Pellegrini, B.A.**[1], **Olwen C. Murphy, M.D.**[1], **Hussein Moussa, M.D.**[1], **Dimitrios Ladakis, M.D.**[1], **Jeffrey Lambe, M.D.**[1], **Kathryn C. Fitzgerald, ScD.**[1], **Lilja Solnes, M.D.**[2], **Arun Venkatesan, M.D., Ph.D.**[1], **Peter A. Calabresi, M.D.**[1], **Shiv Saidha, MBBCh.**[1], **John C. Probasco, M.D.**[1,3]

[1]Division of Neuroimmunology and Neurological Infections, Department of Neurology, Johns Hopkins University School of Medicine, Baltimore, MD, United States.

[2]Russell H. Morgan Department of Radiology and Radiological Sciences, Johns Hopkins University School of Medicine, Baltimore, MD, United States.

[3]Division of Advanced Clinical Neurology, Department of Neurology, Johns Hopkins University School of Medicine, Baltimore, MD, United States.

Keywords

autoimmune encephalitis; anti-NMDA receptor encephalitis; visual function; optical coherence tomography; PET

Corresponding author: John C. Probasco, M.D., Associate Professor of Neurology, Division of Neuroimmunology and Neurological Infections, Division of Advanced Clinical Neurology, Department of Neurology, Johns Hopkins University School of Medicine, 600 N. Wolfe St., Baltimore, MD 21287, United States. Tel: (410) 955-8174, Fax: (410) 955-0672, jprobas1@jhmi.edu.

Statement of Authorship

-Conception and design:
Grigorios Kalaitzidis, M.D, Angeliki Filippatou, M.D., Arun Venkatesan, M.D., Ph.D., Peter A. Calabresi, M.D., Shiv Saidha, MBBCh, John C. Probasco, M.D.

-Acquisition of data:
Grigorios Kalaitzidis, M.D, Angeliki Filippatou, M.D., Nicholas Fioravante, Bsc, Alissa Rothman, M.D, Elias S. Sotirchos, M.D., Eleni Vasileiou, M.D., Henrik Ehrhardt, MBBCh., MSc., Agustina Quiroga, B.A, Nicole Pellegrini, B.A, Olwen C. Murphy, M.D., Hussein Moussa, M.D., Dimitrios Ladakis, M.D., Jeffrey Lambe, M.D., Lilja Solnes M.D.

-Analysis and interpretation of data:
Grigorios Kalaitzidis, M.D, Angeliki Filippatou, M.D., Kathryn C. Fitzgerald, ScD., Arun Venkatesan, M.D., Ph.D., Peter A. Calabresi, M.D., Shiv Saidha, MBBCh, John C. Probasco, M.D.

-Drafting the manuscript:
Grigorios Kalaitzidis, M.D, John C. Probasco, M.D., Arun Venkatesan, M.D., Ph.D., Peter A. Calabresi, M.D., Shiv Saidha, MBBCh

-Revising the manuscript for intellectual content:
Grigorios Kalaitzidis, M.D, John C. Probasco, M.D., Arun Venkatesan, M.D., Ph.D., Peter A. Calabresi, M.D., Shiv Saidha, MBBCh

-Final approval of the completed manuscript:
Grigorios Kalaitzidis, M.D, Angeliki Filippatou, M.D., Nicholas Fioravante, Bsc, Alissa Rothman, M.D, Elias S. Sotirchos, M.D., Eleni Vasileiou, M.D., Henrik Ehrhardt, MBBCh., MSc., Agustina Quiroga, B.A, Nicole Pellegrini, B.A, Olwen C. Murphy, M.D., Hussein Moussa, M.D., Dimitrios Ladakis, M.D., Jeffrey Lambe, M.D., Lilja Solnes M.D., Kathryn C. Fitzgerald, ScD., Arun Venkatesan, M.D., Ph.D., Peter A. Calabresi, M.D., Shiv Saidha, MBBCh, John C. Probasco, M.D.

Introduction

Autoimmune encephalitis (AE) constitutes a discrete subgroup of acute encephalitis, characterized by autoantibody-mediated or other pathogenic immunological mechanisms. AE presents clinically with subacute onset of progressive deficits in working memory, alteration of mental status, seizures and/or new psychiatric symptomatology, typically accompanied by paraclinical features supportive of central nervous system inflammation (EEG, MRI, FDG-PET and/or CSF analysis).[1] Distinct neuronal autoantibodies are associated with distinct syndromes of AE, serving as clinically relevant diagnostic biomarkers. Antigenic targets of AE-associated autoantibodies include intracellular as well as neuronal surface proteins, ion-channels, and receptors.[2]

Anti-NMDA receptor (NMDAR) encephalitis, the most common AE syndrome, has been reported to be associated with post-recovery visual dysfunction.[2] However, optical coherence tomography (OCT) has not demonstrated retinal layer thinning, suggesting that no retinal structural abnormalities could explain the visual dysfunction observed in anti-NMDAR, and that different parts of the visual pathway may be involved.[3] On the other hand, 18F-fluorodeoxyglucose (FDG) PET performed in the acute phase of illness has revealed a pattern of occipital lobe hypometabolism that may be characteristic for anti-NMDAR compared to other AE syndromes and may be more profound among anti-NMDAR patients with the greatest disability.[4]

In the current study, we sought to assess patients with anti-NMDAR encephalitis for evidence of visual dysfunction during outpatient follow-up and the relationship of such visual dysfunction with OCT-identified retinal structure as well as FDG-PET/CT occipital lobe metabolism during the acute phase of illness. Finally, we assessed if acute-phase occipital lobe hypometabolism is associated with subsequent retrograde trans-synaptic degeneration of retinal ganglion cells, as assessed by OCT.[5]

Methods

Standard protocol approvals, registrations, and patient consents

Johns Hopkins University Institutional Review Board approval was obtained for the study. Written informed consent was obtained from all participants prior to study enrolment.

Study participants and clinical data

In this cross-sectional study, patients with anti-NMDAR encephalitis were prospectively recruited from the Johns Hopkins Encephalitis Center outpatient clinic and were invited to undergo OCT and visual function testing. Anti-NMDAR patients were diagnosed according to the consensus clinical criteria, and they were all defined by the detection of serum and/or CSF anti-NMDAR autoantibodies by commercially available assays (Athena Diagnostics, Worcester, MA; Mayo Clinic Laboratories, Rochester, MN).[1] Anti-NMDAR patients were matched to healthy controls (HC) according to age, sex and race, in a ratio of 1:2. Matched HC were identified from an ongoing prospective observational OCT study at our center, and consisted of Johns Hopkins University staff and patients' spouses.

After review of medical records, the following data were collected: demographic information; co-morbidities; diagnosis of co-existing neoplasm(s); diagnostic test results, including antibody assay results; modified Rankin Scale (mRS) scores, representing neurological disability; availability of FDG-PET/CT within 90 days of symptom onset.

Visual function

Monocular and binocular, habitual-corrected visual acuity (VA) was tested using standardized retro-illuminated eye charts (Precision Vision, La Salle, IL). High-contrast VA (100%) and low contrast VA (2.5% and 1.25%) were assessed using the Early Treatment Diabetic Retinopathy Study (ETDRS) chart (at 4 m) and low-contrast Sloan Letter charts (at 2 m), respectively. High-contrast letter-acuity (HCLA) and low-contrast letter-acuity (LCLA) scores were determined by the total number of letters correctly identified on each level of contrast. The maximum score of detectable letters for each chart was 70 (corresponding to a 20/10 Snellen VA).

OCT

Spectral-domain OCT (Cirrus HD-OCT, Model 5000, software version 11.5; Carl Zeiss Meditec, Dublin, CA) was used for retinal imaging, as previously described.[6] Two types of scans were acquired from each participant: Peripapillary scans, using the Optic Disc Cube 200 × 200 protocol, and macular volume scans, using the Macular Cube 512 × 128 protocol. Scans were acquired by experienced technicians, and only scans meeting the OSCAR-IB quality control criteria were included in analyses.[7]

For peripapillary scans, average peri-papillary retinal nerve fiber layer (pRNFL) thickness was estimated using the incorporated software provided by the Cirrus HD-OCT device. For macular scans, automated macular segmentation was performed, as described elsewhere.[8] For each macular layer, the average thickness was obtained within a fovea centered annulus, with an internal diameter of 1 mm and an external diameter of 5 mm. Segmented macular volume scans underwent qualitative assessment in a blinded manner, for the assurance of segmentation accuracy and the recording of retinal pathology (GK, AQ).

Brain FDG-PET/CT

For patients with available FDG-PET/CT performed within 90 days of symptom onset (acute-phase), a review was performed by a board certified nuclear medicine radiologist (LS) using the commercially available database, CortexID (GE Healthcare, Waukesha, WI) as described elsewhere.[4] Briefly, standard CortexID brain regions of interest (ROI) (visual cortex-representing the medial occipital lobe, occipital lobe-representing the lateral occipital lobe, caudate, cerebellum, frontal lobe, parietal lobe, and temporal lobe) were qualitatively assessed as normal, hypo-, or hypermetabolic after visual inspection. In addition, ROIs were semi-quantitatively assessed using the calculated regional average Z-scores using the CortexID database of HC. Because CortexID expresses these Z-scores in terms of hypometabolism, these were corrected to a hypermetabolism scale by multiplying by −1. Thus, corrected regional Z-scores greater than 2.00 or less than −2.00 (i.e., ± 2 SD from the mean of HC for each ROI) were designated as hypermetabolic or hypometabolic, respectively.

Visual function testing, OCT, and FDG-PET/CT timeline

VA testing and OCT were performed at the same follow-up date, at least one year after the acute clinical episode. The specific timing allowed us to: i) search for characteristic patterns of retinal damage in the context of visual dysfunction, ii) seek for evidence of subsequent retrograde trans-synaptic degeneration of retinal ganglion cells following acute occipital hypometabolism,[5] iii) limit the effect of cognitive dysfunction on VA.

Statistical methods

For the comparison of VA and OCT measures between anti-NMDAR and matched HC, mixed-effects linear regression models with subject-specific random intercepts adjusted for age, sex, and race were fitted, accounting for within-subject, inter-eye correlations. Spearman's correlation was used to examine the correlation of medial (visual cortex) and lateral occipital lobe PET Z-scores with VA scores and OCT layer thicknesses.

For FDG-PET Z-score analyses, left and right hemisphere scores were averaged. Likewise, for Spearman's correlation between PET Z-scores and VA, as well as OCT, binocular VA and average OCT layer thicknesses were used.

Statistical analyses were completed using Stata version 16 (StataCorp, College Station, TX, USA). P-value for significance was defined as <0.05.

Data availability

Anonymized data used in this study will be made available upon reasonable request and the proper data sharing agreements in place.

Results

16 anti-NMDAR (32 eyes) and 32 HC (64 eyes) were included in the study (Table 1). Thirteen anti-NMDAR (81%) had mRS ≤ 2 at the time of VA (Table 1).

Visual function and OCT measures in anti-NMDAR compared to HC

Visual function measures and OCT-measured retinal layer thicknesses are summarized and compared between anti-NMDAR and HC in Table 2.

Anti-NMDAR patients had lower LCLA compared to HC, both at 2.5% contrast (− 4.4 letters [95%CI; −8.5 to −0.3] p = 0.04; see Figure, Supplemental Digital Content 1) and 1.25% contrast (−6.8 letters [95%CI; −12.0 to −1.7]; p=0.01; see Figure, Supplemental Digital Content 1). No difference was noted in HCLA between anti-NMDAR patients and HC.

Even though anti-NMDAR patients exhibited worse low-contrast VA compared to HC, no differences were noted for any of the OCT measured retinal layer thicknesses (Table 2, see Figure - Supplemental Digital Content 2).

FDG-PET/CT and its association with Visual function

For anti-NMDAR patients with available acute-phase PET-FDG/CT scans (n = 7), ROI z-scores and number of patients with occipital lobe hypometabolism, as well as the timeline of FDG-PET/CT, OCT, and VA, are summarized in Table 3. Of note, anti-NMDAR patients demonstrated marked lateral and medial occipital hypometabolism relative to other ROIs.

No correlation was noted between acute-phase occipital lobe FDG-PET/CT Z scores and post-recovery letter-acuity scores in the anti-NMDAR patients (Figure 1). In detail, no correlation was found between medial occipital lobe metabolism and 100% contrast VA ($r = -0.36$; $p = 0.43$; Figure 1A), 2.5% contrast VA ($r = -0.31$; $p = 0.50$; Figure 1B) or 1.25% contrast VA ($r = -0.34$; $p = 0.45$; Figure 1C). Similarly, no correlation was found between lateral occipital lobe metabolism and 100%, 2.5%, or 1.25% contrast VA (Figure 1D, 1E, 1F).

FDG-PET/CT association with OCT

No correlation was found between acute-phase occipital lobe PET Z-scores and GCIPL thickness at a time when retrograde trans-synaptic degeneration mediated GCIPL thinning would be evident (Figure 2).

Conclusions

In this study, we aimed to assess the presence of visual dysfunction and characterize the parts of the visual pathway involved in anti-NMDAR encephalitis. Even though post-recovery LCLA was lower in anti-NMDAR patients, we did not find any retinal structural abnormalities on OCT, nor any correlations of acute-phase occipital cortex metabolism on FDG-PET/CT with subsequent visual dysfunction. Occipital lobe metabolism within three months of symptom onset did not correlate with follow-up GCIPL thickness at a time point when retrograde trans-synaptic degeneration would theoretically have been expected to have occurred.

Visual dysfunction following anti-NMDAR encephalitis has been previously described.[3,9,10] When assessing visual function in our study, only low contrast VA was lower in anti-NMDAR patients compared to HC in the post-recovery period. Despite the observation that 81% of anti-NMDAR patients had realized a good neurologic disability outcome by the time of VA and OCT assessment, it is possible that low contrast VA impairment was simply a function of persistent cognitive impairment, as mRS is a poor marker of neurobehavioral outcomes.[11]

Besides cognitive impairment, two parts of the visual system could explain post-recovery visual dysfunction in patients with anti-NMDAR encephalitis. Firstly, the anterior visual pathway spanning from the retina to the thalamic lateral geniculate nucleus. Consistent with prior observations, we found no differences in OCT retinal thicknesses between anti-NMDAR and HC, suggesting that no structurally damaging process is responsible for the noted residual visual dysfunction.[3] However, considering that various types of contrast-modulating retinal neurons express NMDAR, and that anti-NMDAR autoantibodies lead to a selective decrease in anti-NMDAR currents by internalization of the receptor but without

affecting synapse numbers, functional retinal changes as a cause of visual dysfunction cannot be ruled out.[12–14] The second potential target is the posterior visual pathway, from the lateral geniculate nucleus to the visual cortex. Concerning the visual cortex, a pattern of occipital lobe hypometabolism with frontotemporal hypermetabolism has been reported for anti-NMDAR patients, with the antero-posterior gradient correlating with severity of disease, and treatment and recovery leading to its normalization.[15,16] In addition, occipital hypometabolism has been reported to be more evident in anti-NMDAR patients compared to other types of AE.[4] In our study, patients with anti-NMDAR encephalitis were again noted to have significant occipital lobe hypometabolism, more so than for other ROIs. Despite the occipital lobe hypometabolism, no association was noted with post-recovery VA in anti-NMDAR.

Retrograde neuronal degeneration, a well-studied phenomenon, represents neuronal apoptosis following axonal injury. Subsequent apoptosis of the next in chain neurons providing afferent input to the neurons undergoing retrograde degeneration describes the phenomenon of retrograde trans-synaptic degeneration.[17] OCT may be an invaluable tool for studying retrograde trans-synaptic degeneration in the visual pathway.[5,17] In retrograde trans-synaptic degeneration of the visual system, lesions in the neurons of the visual cortex can lead to retinal ganglion cell degeneration, which can be captured on OCT as GCIPL thinning. In our study, FDG-PET/CT occipital lobe hypometabolism did not associate with OCT measured GCIPL thickness, suggesting the absence of retrograde trans-synaptic degeneration mechanisms in anti-NMDAR encephalitis. Anti-NMDAR autoantibodies target neuronal surface proteins and thus potentially lead to reversible functional changes. Functional, short-lasting abnormalities of the visual cortex rather than degenerating mechanisms could explain why FDG-PET/CT occipital hypometabolism did not associate with follow-up OCT measured GCIPL thickness, emphasizing the potential role of immunotherapies in reversing observed dysfunction during the acute-phase of illness.

Our study is limited in several aspects. First, our observations were derived from a relatively small, heterogenous group of patients evaluated at a tertiary, subspecialty clinic. However, anti-NMDAR encephalitis is a rare disease, with a prevalence as low as 0.6 cases per 100,000 per year.[18] Also, patients included in the study were recruited in a single center, and underwent scanning on the same OCT and PET devices, limiting measurement bias. Second, our study is limited by the cross-sectional design. The lack of longitudinal OCT data limited our ability to study dynamic changes of OCT retinal thicknesses in different syndromes of AE and the association of OCT measures with FDG-PET/CT occipital metabolism throughout time. Finally, our study is limited by the retrospective nature of our data.

In conclusion, anti-NMDAR patients exhibit visual dysfunction without structural retinal damage. While occipital hypometabolism could explain visual dysfunction in patients with anti-NMDAR encephalitis, we did not find such an association when comparing acute-phase occipital metabolism with post-acute visual acuity and OCT. Future prospective studies with the addition of acute-phase OCT and VA assessment (if possible), post-acute FDG-PET/CT assessments at time of post-acute OCT and VA assessment, electroretinography, and visual evoked potentials may further clarify visual dysfunction in anti-NMDAR encephalitis.

Supplementary Material

Refer to Web version on PubMed Central for supplementary material.

Funding

This work was supported by the National Institute of Neurological Disorders and Stroke under the grant R01NS082347.

Disclosures

GK, AF, NF, AR, EV, HE, OCM, JL, AQ, NP, HM, DL, KCF, LS report no disclosures.

ESS has served on scientific advisory boards for Viela Bio, Alexion, and Genentech, and has received speaker fees from Viela Bio and Biogen.

AV has received grants from the NIH, Howard Hughes Medical Institute, National Multiple Sclerosis Society, and the Maryland Stem Cell Research Foundation.

PAC has received consulting fees from Disarm and Biogen and is PI on grants to JHU from Biogen and Annexon.

SS has received consulting fees from Medical Logix for the development of CME programs in neurology, and has served on scientific advisory boards for Biogen, Genzyme, Genentech Corporation, EMD Serono, and Celgene. He is the PI of investigator-initiated studies funded by Genentech and Biogen, was the site investigator of a trial sponsored by MedDay Pharmaceuticals and received support from the Race to Erase MS foundation. He has consulted for Carl Zeiss Meditec, and has received equity compensation for consulting from JuneBrain LLC, a retinal imaging device developer.

JCP serves on the editorial board, is an Associate Editor of *The Neurohospitalist*, and is the Editor-in-Chief of *NEJM Journal Watch Neurology*

References

1. Graus F, Titulaer MJ, Balu R, Benseler S, Bien CG, Cellucci T, Cortese I, Dale RC, Gelfand JM, Geschwind M, Glaser CA, Honnorat J, Hoftberger R, Iizuka T, Irani SR, Lancaster E, Leypoldt F, Pruss H, Rae-Grant A, Reindl M, Rosenfeld MR, Rostasy K, Saiz A, Venkatesan A, Vincent A, Wandinger KP, Waters P, Dalmau J. A clinical approach to diagnosis of autoimmune encephalitis. Lancet Neurol. 2016;15(4):391–404. [PubMed: 26906964]
2. Dalmau J, Graus F. Antibody-mediated encephalitis. N Engl J Med. 2018;378(9):840–851. [PubMed: 29490181]
3. Brandt AU, Oberwahrenbrock T, Mikolajczak J, Zimmermann H, Pruss H, Paul F, Finke C. Visual dysfunction, but not retinal thinning, following anti-NMDA receptor encephalitis. Neurol Neuroimmunol Neuroinflamm. 2016;3(2):e198. [PubMed: 26894203]
4. Probasco JC, Solnes L, Nalluri A, Cohen J, Jones KM, Zan E, Javadi MS, Venkatesan A. Decreased occipital lobe metabolism by FDG-PET/CT: An anti-NMDA receptor encephalitis biomarker. Neurol Neuroimmunol Neuroinflamm. 2017;5(1):e413. [PubMed: 29159205]
5. Jindahra P, Petrie A, Plant GT. The time course of retrograde trans-synaptic degeneration following occipital lobe damage in humans. Brain. 2012;135(Pt 2):534–541. [PubMed: 22300877]
6. Syc SB, Warner CV, Hiremath GS, Farrell SK, Ratchford JN, Conger A, Frohman T, Cutter G, Balcer LJ, Frohman EM, Calabresi PA. Reproducibility of high-resolution optical coherence tomography in multiple sclerosis. Mult Scler. 2010;16(7):829–839. [PubMed: 20530512]
7. Tewarie P, Balk L, Costello F, Green A, Martin R, Schippling S, Petzold A. The OSCAR-IB consensus criteria for retinal OCT quality assessment. PLoS One. 2012;7(4):e34823. [PubMed: 22536333]
8. Lang A, Carass A, Hauser M, Sotirchos ES, Calabresi PA, Ying HS, Prince JL. Retinal layer segmentation of macular OCT images using boundary classification. Biomed Opt Express. 2013;4(7):1133–1152. [PubMed: 23847738]

9. Cobo-Calvo A, Izquierdo Gracia C, Quinones SM, Torro CM, Saiz A, Dalmau J, Martinez-Yelamos S. Optic neuritis in the setting of NMDA receptor encephalitis. J Neuroophthalmol. 2014;34(3):316–319. [PubMed: 24905275]

10. Sawamura H, Yamamoto T, Ohtomo R, Bannai T, Wakakura M, Tsuji S. Anti-NMDA receptor encephalitis associated with transient cerebral dyschromatopsia, prosopagnosia, and lack of stereopsis. J Neuroophthalmol. 2014;34(2):144–148. [PubMed: 24647141]

11. Yeshokumar AK, Gordon-Lipkin E, Arenivas A, Cohen J, Venkatesan A, Saylor D, Probasco JC. Neurobehavioral outcomes in autoimmune encephalitis. Journal of neuroimmunology. 2017;312:8–14. 10.1016/j.jneuroim.2017.08.010. doi: 10.1016/j.jneuroim.2017.08.010. [PubMed: 28889962]

12. Eliasof S, Jahr CE. Rapid AMPA receptor desensitization in catfish cone horizontal cells. Vis Neurosci. 1997;14(1):13–18. [PubMed: 9057264]

13. Diamond JS, Copenhagen DR. The contribution of NMDA and non-NMDA receptors to the light-evoked input-output characteristics of retinal ganglion cells. Neuron. 1993;11(4):725–738. [PubMed: 8104431]

14. Hensley SH, Yang XL, Wu SM. Identification of glutamate receptor subtypes mediating inputs to bipolar cells and ganglion cells in the tiger salamander retina. J Neurophysiol. 1993;69(6):2099–2107. [PubMed: 7688801]

15. Yuan J, Guan H, Zhou X, Niu N, Li F, Cui L, Cui R. Changing brain metabolism patterns in patients with ANMDARE: Serial 18F-FDG PET/CT findings. Clin Nucl Med. 2016;41(5):366–370. [PubMed: 26914566]

16. Chen B, Wang Y, Geng Y, Huang Y, Guo S, Mao X. Marked improvement of anti-N-methyl-D-aspartate receptor encephalitis by large-dose methylprednisolone and plasmapheresis therapy combined with (18)F-fluorodeoxyglucose positron emission tomography imaging: A case report. Exp Ther Med. 2014;8(4):1167–1169. [PubMed: 25187817]

17. Dinkin M Trans-synaptic retrograde degeneration in the human visual system: Slow, silent, and real. Curr Neurol Neurosci Rep. 2017;17(2):16–2. [PubMed: 28229400]

18. Dubey D, Pittock SJ, Kelly CR, McKeon A, Lopez-Chiriboga AS, Lennon VA, Gadoth A, Smith CY, Bryant SC, Klein CJ, Aksamit AJ, Toledano M, Boeve BF, Tillema JM, Flanagan EP. Autoimmune encephalitis epidemiology and a comparison to infectious encephalitis. Ann Neurol. 2018;83(1):166–177. [PubMed: 29293273]

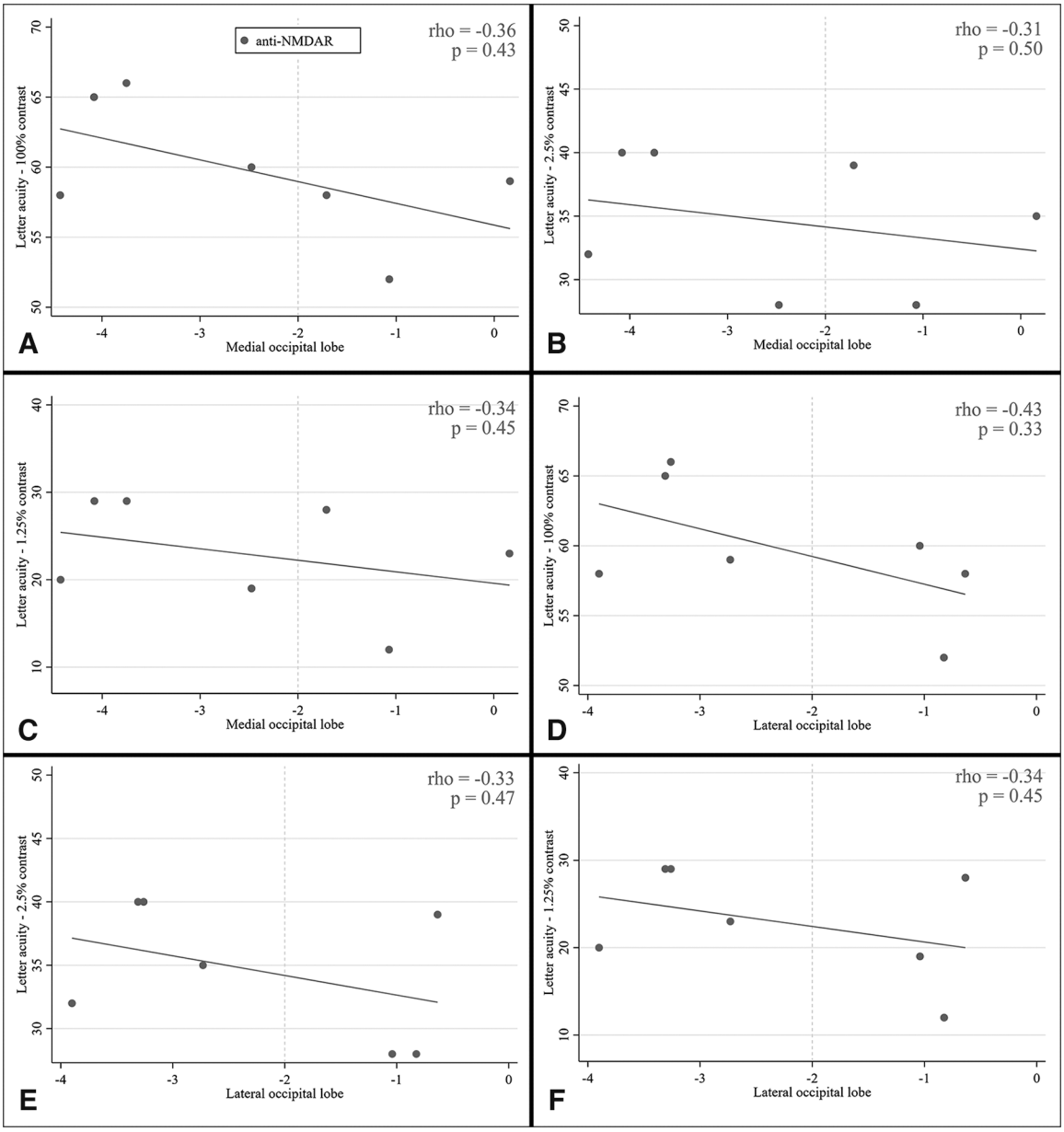

Figure 1. Relationships between follow-up letter-acuity scores and acute onset FDG-PET/CT medial and lateral occipital lobe Z-scores in anti-NMDAR.

Two-way scatter plots depicting the lack of an association between acute-phase medial occipital lobe FDG-PET/CT Z-scores and letter-acuity scores for anti-NMDAR at all contrasts (A. 100% contrast, B. 2.5% contrast and C. 1.25% contrast), as well as the lack of an association between acute-phase lateral occipital lobe FDG-PET/CT Z-scores and letter-acuity scores at all contrasts (D. 100% contrast, E. 2.5% contrast and F. 1.25% contrast). Spearman's correlation coefficients and relative p-values are also reported. The vertical, dashed, gold line represents the tipping point in terms of hypometabolism – when FDG-PET/CT Z-scores are lower than −2 the ROI is considered to be hypometabolic.

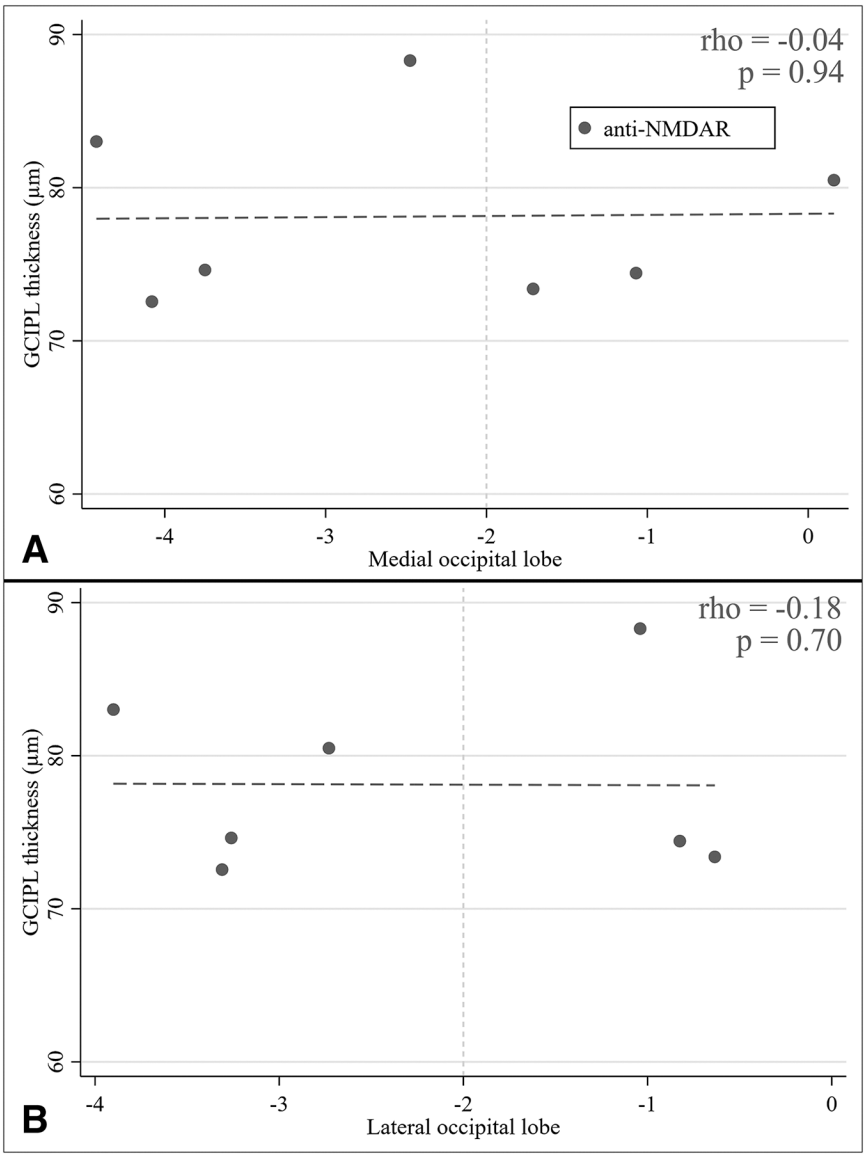

Figure 2. Relationships between follow-up GCIPL thickness and acute onset medial and lateral occtipital lobe FDG-PET/CT Z-scores in anti-NMDAR.

Two-way scatter plots depicting the lack of an association between acute-phase occipital lobe FDG-PET/CT Z-scores (A. medial, B. lateral occipital lobe) with GCIPL thickness. Spearman's correlation coefficients and relative p-values are also reported. The vertical, dashed, gold line represents the tipping point in terms of hypometabolism – when FDG-PET/CT Z-scores are lower than −2 the ROI is considered to be hypometabolic.

Table 1.

Demographic and clinical characteristics of participants

	Anti-NMDAR	HC
Participants, n (eyes)	16 (32 eyes)	32 (64 eyes)
Age in years, mean (SD)	30.6 (12.2)	30 (11.1)
Female sex, n (%)	13 (81%)	26 (81%)
Race, n (%)		
Caucasian American	9 (56%)	18 (56%)
African American	4 (25%)	8 (25%)
Other	3 (19%)	6 (19%)
New cancer diagnosis, n (%)	6 (38%)	
Ovarian Teratoma	4 (25%)	
Diffuse large B cell lymphoma	1 (6%)	
Melanoma	1 (6%)	
mRS ≤ 2 at the time of VA, n (%)	13 (81%)	

NMDAR: NMDA receptor; **HC**: Healthy control; **SD**: Standard deviation; **mRS**: Modified Rankin Scale

Table 2.

Summary and comparison of letter acuity scores and optical coherence tomography retinal layer thicknesses

	Anti-NMDAR	HC	Anti-NMDAR vs HC	
Letter-acuity scores, median (IQR)			**Beta (95% CI)[a]**	**P-value[a]**
100% contrast	56.5 (53 to 61.5)	60 (56 to 64)	−2.6 (−6.4 to 1.2)	0.18
2.5% contrast	29 (22 to 35)	34 (26.5 to 37)	−4.4 (−8.5 to −0.3)	**0.037**
1.25% contrast	12.5 (4 to 22)	22 (14.5 to 27.5)	−6.8 (−12.0 to −1.7)	**0.010**
OCT measures, μm, mean (SD)				
GCIPL	74.6 (6.1)	75.5 (3.8)	−0.8 (−3.5 to 1.8)	0.54
INL	44.6 (1.9)	44.1 (2.0)	0.5 (−0.6 to 1.6)	0.36
ONL	66.2 (3.6)	67.1 (5.4)	−0.9 (−3.7 to 1.9)	0.52
AMT	307.6 (11.3)	309.4 (10.8)	−1.7 (−7.7 to 4.3)	0.58
pRNFL	90.2 (12.2)	94.1 (9.0)	−3.9 (−9.4 to 1.5)	0.16

NMDAR: NMDA receptor; **HC**: Healthy control; **IQR**: Interquartile range; **SD**: Standard deviation; **GCIPL**: Ganglion cell/Inner plexiform layer; **INL**: Inner Nuclear layer; **ONL**: Outer Nuclear layer; **AMT**: Average Macular thickness; **pRNFL**: Peripapillary Retinal Nerve Fiber layer.

[a]Mixed-effects linear regression models adjusted for age, sex and race were used in analyses. Beta coefficients represent differences in number of correct letters and micrometers between the groups compared, for letter-acuity scores and OCT measures, respectively. Statistically significant results are in bold.

Table 3.

Summary of regional FDG-PET/CT metabolism within 3 months of symptom onset for NMDA receptor, and FDG-PET/CT, VA, and OCT timeline.

Region	Anti-NMDAR
N (patients)	7
PET–FDG/CT Z–scores, median (IQR)	
Lateral occipital lobe	−2.7 (−3.3 to −0.8)
Visual cortex (medial occipital cortex)	−2.5 (−4.1 to −1.1)
Parietal lobe	−1.0 (−2.9 to −0.2)
Temporal lobe	−1.1 (−1.6 to 0.2)
Frontal lobe	−1.4 (−2.4 to 0.2)
Caudate	−1.0 (−3.0 to 2.0)
Cerebellum	−0.0 (−0.9 to 1.8)
N of abnormal cortical metabolism on semi-quantitative assessment (patients)	
Occipital lobe (medial and/or lateral) hypometabolism	5 (71%)
Time between FDG−PET/CT and onset, days (range)	26 (15 to 52)
Time between FDG−PET/CT and VA/OCT, days (range)	620 (491 to 705)
Time between VA/OCT and onset, days (range)	635.5 (71 to 3,860)